Acta Crystallographica Section A
Foundations of Crystallography
ISSN 0108-7673

Received 5 February 2005
Accepted 23 April 2005

Growth process of the ridge–trough faces of a twinned crystal

Jae-Wook Lee,[a]* Ui-Jin Chung,[b] Nong M. Hwang[c] and Doh-Yeon Kim[c]

[a]Korea Institute of Machinery and Materials, 66 Sangnam-dong, Changwon, Kyungnam 641-010, South Korea, [b]Samsung Electronics Co., Yongin, Kyunggi 449-711, South Korea, and [c]Center for Microstructure Science of Materials, School of Materials Science and Engineering, Seoul National University, Bldg 37, Rm 106, Seoul 151-742, South Korea. Correspondence e-mail: jaewook@kmail.kimm.re.kr

For a twinned face-centered-cubic crystal, the energy barrier for two-dimensional nucleation on a concave trough (or a re-entrant edge) and that for a layer advancing across a convex ridge were calculated. The former was obtained by analyzing the line tension of the trough. The results show that their energy barriers are 39 and 50% compared to that for nucleation on a flat {111} face, respectively. Therefore, the layer advance across the ridge is found to be more difficult than the nucleation on the trough. Based on these results, the morphology of the growing surface is predicted and an alternative growth process by the twin-plane-re-entrant-edge mechanism is suggested.

1. Introduction

When single crystals are grown from the melt, it is well known that twinned seed crystals grow very rapidly compared to normal ones (Berriman & Herz, 1957; Hamilton & Brady, 1964). Furthermore, the crystal morphologies obtained from twinned seeds are unique such as *V*-shaped quartz (Sunagawa & Yasuda, 1983; Sunagawa, 1987), tabular or elongated AgBr (Berriman & Herz, 1957) and star-shaped Si (Pei & Hosson, 2001). Therefore, the growth process of twinned crystals has been the subject of many researches (Hamilton & Seidensticker, 1960; Wagner, 1960; Jagannathan *et al.*, 1993; Bögels *et al.*, 1997; Lee *et al.*, 2003). Recently, a similar phenomenon was also reported to occur during the grain coarsening process of polycrystalline ceramics. The abnormally grown large $BaTiO_3$ and $Pb(Mg_{1/3}Nb_{2/3})O_3$–35 mol% $PbTiO_3$ grains were determined to have twins and their shapes were similar to those of AgBr and Si twinned crystals, respectively (Yoo *et al.*, 1994; Chung *et al.*, 2002).

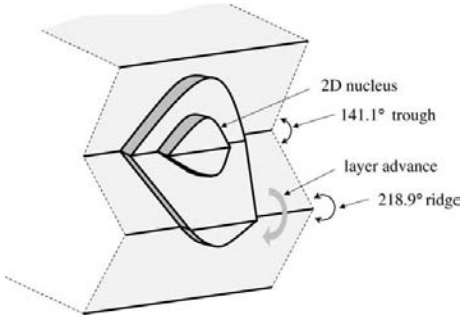

Figure 1
Schematic showing the ridge–trough side face of a doubly twinned crystal.

The growth advantage of a twinned crystal has been explained mainly in terms of a ridge–trough face structure (Berriman & Herz, 1957). Fig. 1 shows the side face of face-centered-cubic (f.c.c.) crystals with two parallel {111} twin planes, which has a 141.1° trough and a 218.9° ridge. This can be denoted as a {111}/{111}/{111} structure, where the three faces indicate those of the upper/middle/lower crystals separated by the {111} twin planes, respectively. Here, the concave trough is known to act as a preferential site for two-dimensional (2D) nucleation so that the growth of a crystal along the direction parallel to the twin plane is enhanced. In particular, when the crystal possesses more than two parallel twin planes (double twins), the trough shown in Fig. 1 is maintained during the growth process so that the crystal can grow continuously at a high rate (Hamilton & Seidensticker, 1960; Wagner, 1960; van de Waal, 1996). This process has been referred to as the twin-plane-re-entrant-edge (TPRE) growth mechanism and supported by various experimental results (Sunagawa, 1987; Uyeda, 1987).

However, there is still some controversy over the enhanced 2D nucleation on the trough. For instance, Li & Ming (1995) claimed that the nucleation-energy barrier on the trough is similar to that on a flat face. On the other hand, Jagannathan *et al.* (1993, 1995) have found a {111}/{100}/{111} structure at the side faces of twinned AgBr crystals, instead of a {111}/{111}/{111} structure. They suggested that the {111}/{111} trough disappears from the surface because the layer advance across the ridge (Fig. 1) is more difficult than the nucleation on the trough. Therefore, the {100} face in the middle crystal was suggested to be the origin of the high growth rate. However, van de Waal (1995) refuted this by showing that an adatom on the trough has the same number of bonds as that at the step on

the ridge. He supported the TPRE mechanism in which the nucleation on the trough is the slowest process.

In this work, we try to provide further understanding on the enhanced growth of a twinned crystal by calculating the energy barriers for the nucleation on the trough and for the layer advance across the ridge. Note that the growth rate is directly related to the height of the energy barrier. For the calculation, a twinned monoatomic f.c.c. crystal was assumed and the atomic interactions were confined to the first nearest neighbors (FNN). The results confirm that the growth rate is effectively enhanced by the presence of twins and the re-entrant edges do not disappear during the process. However, the overall growth process is determined to be different from that predicted earlier by the TPRE mechanism.

2. 2D nucleation on a flat face

When a circular 2D nucleus is formed on a flat surface, the free-energy change (ΔG_{2D}) can be described as

$$\Delta G_{2D} = \pi r^2 \Delta\mu + 2\pi r\varepsilon, \tag{1}$$

where r is the radius of the nucleus, $\Delta\mu$ is the driving force for growth and ε is the step energy. Note that equation (1) is a two-dimensional description, *i.e.* a black circle on white paper is assumed instead of a disc on a flat face. The volume of the nucleus is not considered and ε is a line energy that does not depend on the step height.

From equation (1), the nucleation barrier (ΔG^*_{2D}) is obtained as

$$\Delta G^*_{2D} = \pi\varepsilon^2/\Delta\mu. \tag{2}$$

Here, $\Delta\mu$ represents the driving force per unit area. Assuming that $\Delta\mu_a$ is the driving force per atom and d is the atomic diameter, then $\Delta\mu = \Delta\mu_a/d^2$ for the {100} surface while $\Delta\mu = 2\Delta\mu_a/3^{1/2}d^2$ for the {111} surface. (Note that, as shown in Fig. 2, one atom occupies d^2 for the {100} surface while one atom occupies $3^{1/2}d^2/2$ for the {111} surface.) Therefore, $\Delta\mu$ at the {111} surface is slightly larger than that at the {100} surface.

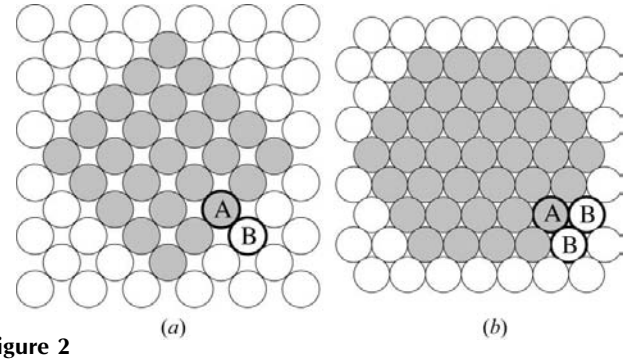

Figure 2
Atomic configurations of (*a*) a {100} and (*b*) a {111} surface of a f.c.c. crystal. Gray circles show a square (*a*) and a hexagonal (*b*) area surrounded by ⟨110⟩ lines. The A atom in the ⟨110⟩ line has one neighboring B atom on the {100} face but two on the {111}, perpendicular to the line direction.

On the other hand, the step energy can be described from the broken-bond model as follows (Gilmer, 1976; Bonzel, 2001):

$$\varepsilon = \varepsilon_0 - 2kT\exp\left(-\frac{\varepsilon_k}{kT}\right) \tag{3}$$

$$= Z^{\perp}\varphi - 2kT\exp\left(-\frac{Z^{\parallel}\varphi}{kT}\right), \tag{4}$$

where k is the Boltzmann constant, T the temperature and φ the bond energy. Note that ε_0 and ε_k are the step energy at 0 K and the kink formation energy, respectively, and $Z^{\parallel}$ and $Z^{\perp}$ are the number of broken bonds parallel and perpendicular to the step direction, respectively. The first term on the right side of equation (3) or (4) is the enthalpic contribution by forming broken bonds and the second term is the configurational entropic one by forming kinks on the step. When the entropic term is ignored by assuming a very low temperature, it reduces to

$$\varepsilon = Z^{\perp}\varphi. \tag{5}$$

The 2D nuclei on the {100} and the {111} faces of the f.c.c. crystals are expected to have ⟨110⟩ steps since the ⟨110⟩ is the most closely packed direction on both faces. Along the ⟨110⟩ direction, the numbers of broken bonds per atom are 1 for {100} and 2 for {111}, as shown in Fig. 2. Therefore, the step energies per unit length on the {100} and the {111} surfaces are φ/d and $2\varphi/d$, respectively. Note that the step energy depends not only on the step direction but also on the crystal face on which the step is formed.

By introducing the driving forces and the step energies into equation (2), the formation energies of a 2D nucleus on the {100} and the {111} faces are obtained as $\pi\varphi^2/\Delta\mu_a$ and $2\times 3^{1/2}\pi\varphi^2/\Delta\mu_a$, respectively. This indicates that the nucleation barrier for the {100} face is approximately 29% of that for the {111} face. Therefore, a significant difference in the growth rates for the {100} and the {111} faces is expected because the rate is proportional to $\exp(-\Delta G^*_{2D}/3kT)$ (Hilling, 1966; van der Eerden, 1993). In this circumstance, an octahedral crystal bounded by the slow-growing {111} faces results, as shown in a previous simulation study (Lee *et al.*, 2003).

3. 2D nucleation on a trough

In order to calculate the energy barrier for 2D nucleation on a trough, the shape of the nucleus first needs to be determined. As shown in Fig. 3, two different shapes were suggested previously (Hamilton & Brady, 1964; Tiller, 1991); the elliptical and the semicircular nuclei. Among them, the nucleus with the lower-energy barrier will be more likely to appear.

3.1. Elliptical 2D nucleus

The energy barrier for 2D nucleation on a trough is proportional to its area ratio compared to the circular one on a flat face and this is in turn determined by the force balance at the intersection. The forces that determine the area of a nucleus are the step energies, ε, and the line energy of the

trough, as indicated in Fig. 3(*a*). (Hereafter, the line energy of the trough will be referred to as *the groove energy*, ε_g.) Here, it is unnecessary to consider the ε_g pointing toward the outside of the nucleus (the dotted arrow in Fig. 3*a*) because only the forces acting on a common point need to be considered. Note that both the step energies and the inward ε_g are due to the atoms that belong to the nucleus and join at the same point. However, the outward ε_g is due to the atoms at a crystal surface and does not meet at the point concerned.

Since the step energy of the {111} face was already obtained, the contact angle, θ in Fig. 3(*a*), can be determined by finding the (inward) ε_g. In fact, ε_g has never been formulated. Therefore, quantitative analysis of the TPRE mechanism could not be made (Li & Ming, 1995; Tiller, 1991). The continuum approach for calculating ε_g from the angle of the trough (Tiller, 1991) appears unreliable because a 2D nucleus has no volume (§2). In this study, therefore, we tried to quantify ε_g through atomistic considerations as in the calculation of the step energy.

During nucleation, each atom composing the ⟨110⟩ step on the {111} face takes three broken bonds from the lower surface but creates three top-broken and two side-broken bonds. Therefore, the energy of the ⟨110⟩ step on the {111} face is $(5\varphi - 3\varphi)/d$ as shown in the previous section. Indeed, the bonds of an atom in the nucleus can be divided into the following three groups; the bonds with atoms at the surface (z_1), those with atoms inside the nucleus (z_2) and those remaining broken after nucleation (z_3). Then, the energy barrier for nucleus formation per atom (ε_a) can be predicted:

$$\varepsilon_a = (z_3 - z_1)\varphi. \qquad (6)$$

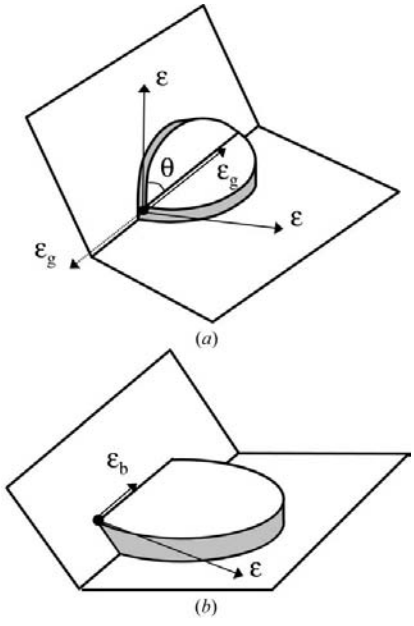

Figure 3
Schematics showing (*a*) an elliptical and (*b*) a semicircular 2D nucleus on the {111}/{111} trough. ε, ε_g and ε_b are the step, the groove and the boundary energies, respectively. θ is the contact angle.

This corresponds to the well known fact that the energy barrier is the change in the number of broken bonds during the formation of a given subject.

The atoms composing the groove are shown in Fig. 4(*a*). Each atom has four bonds with the surface-layer atoms (z_1), six with the atoms in the nucleus itself (z_2) and two broken bonds to the surface (z_3). In total, it has 12 bonds, which is equivalent to the coordination number of the f.c.c. structure. From equation (6), ε_g was found to be $(2\varphi - 4\varphi)/d$. Note that it has a *negative* value, which means that ε_g acts outward from the nucleus, even though it lies on the inside of the nucleus. The direction of ε_g shown in Fig. 4(*a*) should be reversed. Thus, ε_g causes the nucleus to elongate along the trough and the area of the nucleus becomes smaller. The growth process by 2D nucleation will therefore be enhanced at the trough.

When $\varepsilon_g = -2\varphi/d$, the force balance makes a contact angle of 60°, as shown in Fig. 4(*b*). The area of this ellipse is $(2\pi/3 - 3^{1/2}/2)r^2$, which corresponds to 39% of that of a circle with the same radius. Therefore, the energy barrier for nucleation on the trough also becomes 39% compared to that on the flat {111} surface, which makes nucleation on the trough much easier. Note that the energy barrier for nucleation on the trough is slightly higher than that on the {100} face calculated in §2.

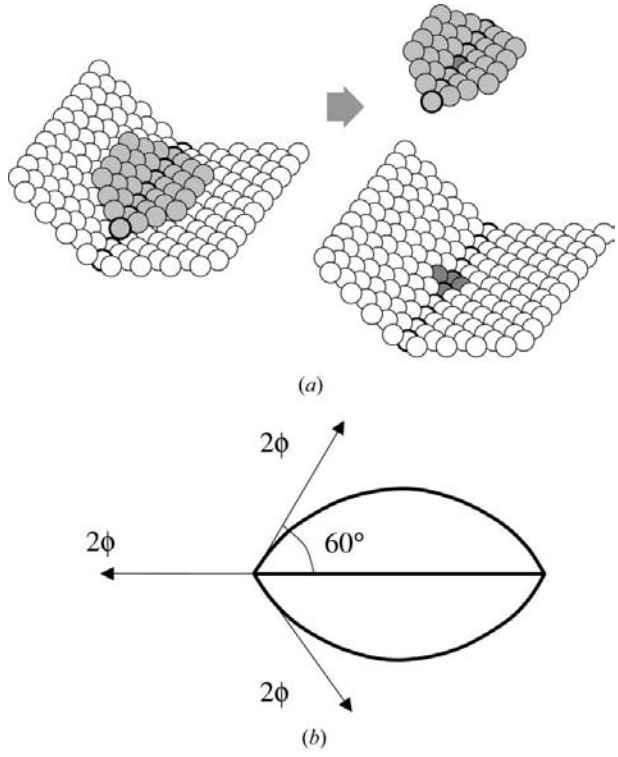

Figure 4
(*a*) Atomic configuration of the elliptical 2D nucleus on the trough and (*b*) its schematic representation showing the force balance. In (*a*), the elliptical 2D nucleus on the trough on the left is divided into the nucleus (gray circles) and the lower layer (white circles) on the right. In the right of (*a*), the atom in the center of the nuclear groove (dark-gray circle) has bonds with four atoms (dark-gray circles) in the lower layer. The circles with bold borders show the atoms forming the grooves.

3.2. Semicircular 2D nucleus

The energy barrier for the formation of a semicircular nucleus can be calculated in the same way. In order to distinguish the line energy of the trough of this semicircular nucleus from that of the elliptical one, we denote it as ε_b (Fig. 3*b*). The atoms forming this boundary are illustrated in Fig. 5(*a*). For each atom, z_1, z_2 and z_3 are all 4. From equation (6) again, ε_b is predicted to be zero, which makes a contact angle of 90°. The nucleus becomes a half-circle as shown in Fig. 5(*b*). This suggests that the energy barrier for the nucleus is 50% of that for the circular one. In this respect, the formation of a semicircular nucleus is less likely than an elliptical one for which the energy barrier is 39% of that for the circular one. The nucleus on the trough is believed to be elliptical in shape.

4. Layer advance across a ridge

The layer advance can be regarded as a one-dimensional nucleation process, as shown in Fig. 6(*a*). When atoms in a straight line are added to the ⟨110⟩ step on a {111} face, one atom in the line takes three broken bonds from the lower surface and two from the pre-existing step. On the other hand, it creates three broken bonds on the top and two broken bonds to the side. Therefore, the number of broken bonds does not change with this layer advance. However, it becomes different when a line is added to the ⟨110⟩ step on the ridge, as shown in Fig. 6(*b*). One atom takes two broken bonds from the surface layer and two from the pre-existing step but it creates four broken bonds on the top and two broken bonds to the side. Therefore, an increase in energy of 2φ is noted, which confirms that there is an energy barrier for the layer advance across the ridge.

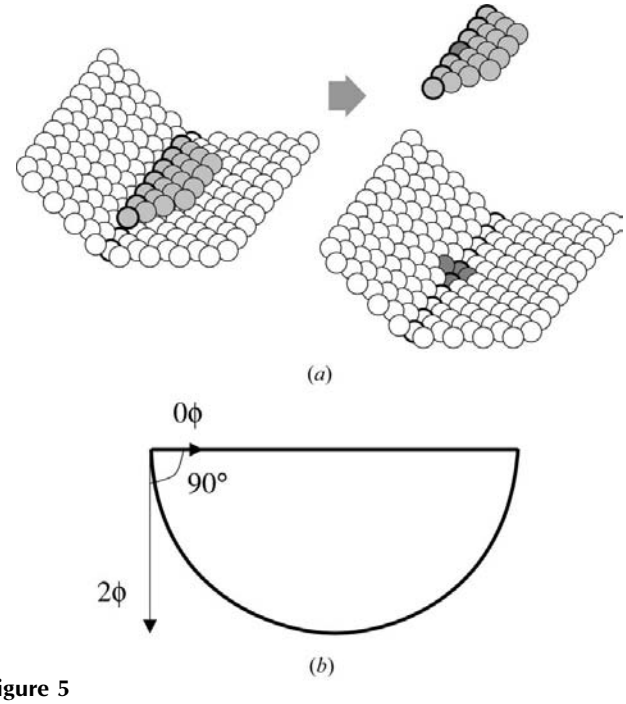

Figure 5
(*a*) Atomic configuration of the semicircular 2D nucleus on the trough and (*b*) its force balance.

In this case, the layer advance is expected to occur by the substep mechanism (Ming *et al.*, 1988; Bögels *et al.*, 1997), which can be regarded as heterogeneous 2D nucleation (Fig. 7). This process is quite similar to the semicircular nucleation on the trough (§3.2). Through the atomic configuration of the line added to the substep (Fig. 8*a*), the line energy (ε_s) and the shape of nucleus can be determined. The z_i values for these atoms are all 4. Incidentally, this is identical to the atoms forming the boundary in the semicircular nucleation on the trough (Fig. 5*a*). Thus, the energy barrier for nucleation at the substep on the ridge is half of that for the circular nucleation on the flat {111} face (Fig. 8*b*). Note that this energy barrier is still higher than that for the elliptical nucleation on the trough. In this respect, the layer advance across the ridge is expected

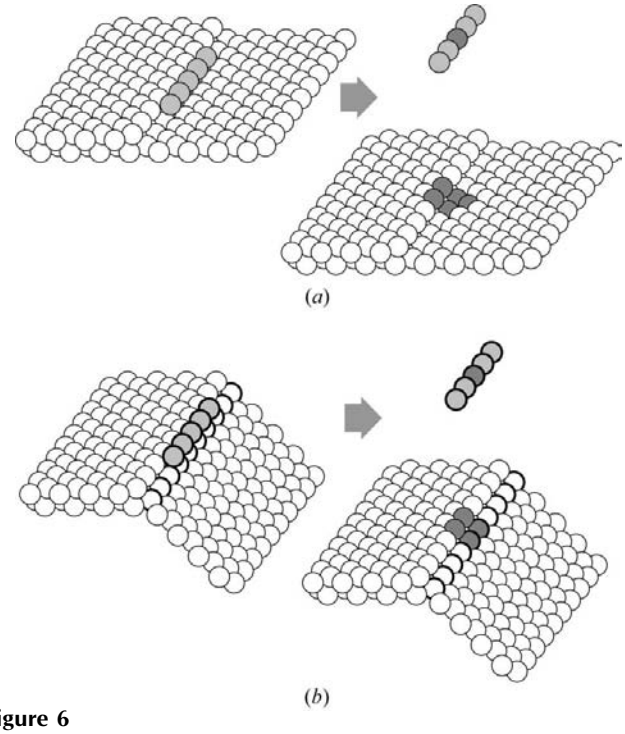

Figure 6
Atomistic description of the addition of an atomic line to the ⟨110⟩ step on (*a*) the {111} face and (*b*) the ridge.

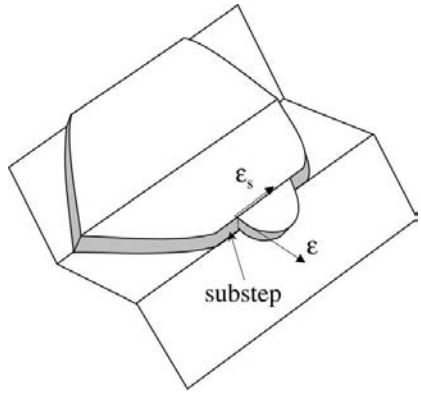

Figure 7
Schematic showing 2D nucleation at the layer edge on the ridge (substep). ε_s is the energy of a line contacting the substep.

to be more difficult than the nucleation on the trough, as suggested earlier (Jagannathan *et al.*, 1993).

As mentioned in the *Introduction*, if the rate of layer advance is lower than the nucleation rate, the layers nucleated on the trough should accumulate around the ridge. As a result, the trough becomes buried and disappears from the surface. However, the computer-simulation results (Lee *et al.*, 2003) indicate that the trough is maintained when only the FNN interaction is included as in this work. This difference suggests that there is an alternative growth mechanism by which the trough can be maintained.

5. Growth process enhanced by TPRE

According to Jagannathan *et al.* (1993), the {100} surface is formed by the edges of accumulated layers, as shown in Fig. 9. The accumulation begins at the vicinity of the ridge (Fig. 9*b*) and, beyond a certain degree of accumulation, the entire surface of the middle crystal is covered (Fig. 9*c*). In this explanation, the {100} surface is assumed to grow at a lower rate than the {111}/{111} trough. Otherwise, the {111}/{111} trough will be maintained.

The growth rate of the {100} face and that of the {111}/{111} trough can be estimated through their nucleation barriers (ΔG^*), which were already calculated to be 29 and 39% of the energy barrier for nucleation on a flat {111} face, respectively. Note that the growth rate as a result of nucleation on a face is proportional to $\exp(-\Delta G^*/3kT)$ while that by nucleation on a line is proportional to $\exp(-\Delta G^*/2kT)$ (Tiller, 1991; van der Eerden, 1993). Therefore, the {100} surface formed by the accumulated layers is expected to grow much faster, which is in contrast to the suggestion by Jagannathan *et al.* The {100} surface of the middle crystal would be too narrow to replace the {111}/{111} trough.

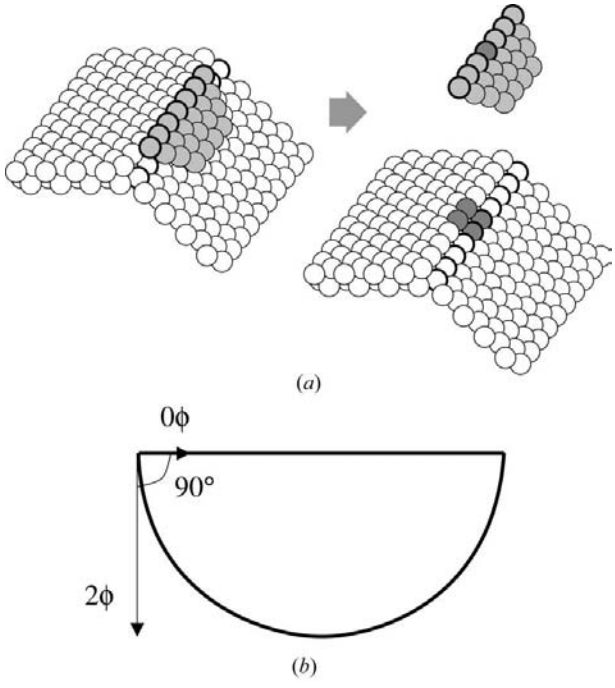

Figure 8
(*a*) Atomic configuration of the semicircular 2D nucleus at the layer edge on the ridge and (*b*) its force balance.

Table 1
The energy barriers for all processes and their percentages with respect to the nucleation on the {111} face.

	Activation barrier	Percentage (%)
Circular nucleus on {111} face	$2 \times 3^{1/2}\pi\varphi^2/\Delta\mu_a$	100
Circular nucleus on {100} face	$\pi\varphi^2/\Delta\mu_a$	29
Elliptical nucleus on trough	$(4 \times 3^{1/2}\pi/3 - 3)\varphi^2/\Delta\mu_a$	39
Semicircular nucleus on trough	$3^{1/2}\pi\varphi^2/\Delta\mu_a$	50
Layer advance across ridge	$3^{1/2}\pi\varphi^2/\Delta\mu_a$	50

Once the layer nucleates on the {100} face of the middle crystal, it can propagate to the lower crystal without any energy barrier. Note that the 218.9° ridge is already replaced with a 164.2° trough, as shown in Fig. 9(*b*). This new trough is expected to increase further the growth rate of the {100} face. In this respect, it is believed that the {100} face grows faster than the {111}/{111} trough, as already discussed.

Table 1 summarizes the energy barriers for all the processes concerned. From this, the overall crystal growth process by the TPRE mechanism is predicted to occur, as shown schematically in Fig. 10. Initially, 2D nucleation occurs on the {111}/{111} trough and the nucleus adopts an elliptical shape (Fig. 10*a*). The nucleated layers grow laterally but cannot cross the ridge. Consequently, a narrow {100} face is formed by the edges of the accumulated layers (Fig. 10*b*). Then, 2D nucleation occurs simultaneously on the {111}/{111} trough and the narrow {100} face, as shown in Fig. 10(*c*). When the nucleation on the {111}/{111} trough is easier, the {100} face becomes wider and nucleation on it is enhanced. In contrast, when the nucleation rate on the {100} face is faster, the {100} face becomes narrower and the nucleation rate on it is reduced. In this way, the {100} face is maintained at a certain level and competes with the {111}/{111} trough. Note that the growth rate of the entire ridge–trough face is still determined by slow nucleation on the {111}/{111} trough. The narrow {100} face in the middle crystal does not alter the growth kinetics of the

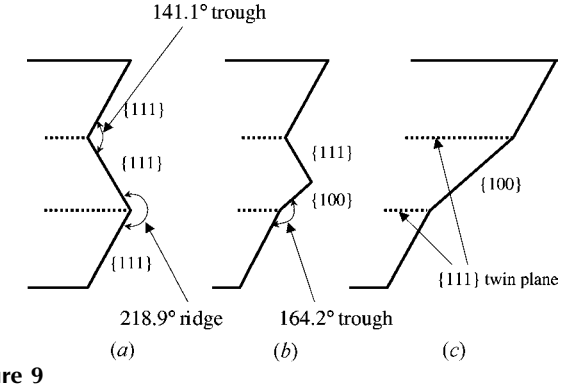

Figure 9
The development of a {100} face in the middle crystal. (*a*) The side face of a twinned crystal has a {111}/{111}/{111} structure initially. (*b*) Layers are accumulated at the ridge and their edges form a {100} face in the middle crystal. (*c*) The {100} face covers the entire face of the middle crystal.

surface but only prevents the {111}/{111} trough from disappearing.

In this regard, the ridge–trough face structure observed in the simulations and experiments does not always mean that the nucleation on the trough is more difficult than the layer advance across the ridge. The trough formed by twinning definitely enhances the growth of the surface. However, without a narrow {100} face in the middle crystal, it would not even exist. The TPRE mechanism, which emphasizes only the role of the trough, should be modified to include the critical role of the {100} face. Note that the cooperation of the trough and the {100} face was already suggested by Ming & Sunagawa (1988), who also developed the substep mechanism illustrated in §§3.2 and 4. But their idea shows how a 70.53° and a 109.47° trough work with a rough {100} face and so is not relevant to this work.

6. Conclusions

By calculating the energy barriers for the 2D nucleation on the trough and for the layer advance across the ridge of the twinned f.c.c. crystals, the layer advance was determined to be more difficult than the nucleation on the trough. Therefore, the nucleated layers should accumulate around the ridge. Nevertheless, the trough is suggested to be maintained because the accumulation is limited to a certain thickness by the formation of a narrow {100} face at the edges. This analysis confirms that the trough (the re-entrant edge) enhances the growth rate of the surface without disappearing. However, the results show that the whole process is not as simple as predicted by the original TPRE mechanism. A new plausible growth process by TPRE was described. The effects of the temperature and the second-nearest-neighbor (SNN) interaction on the energy barrier will be reported elsewhere (Lee *et al.*, 2005).

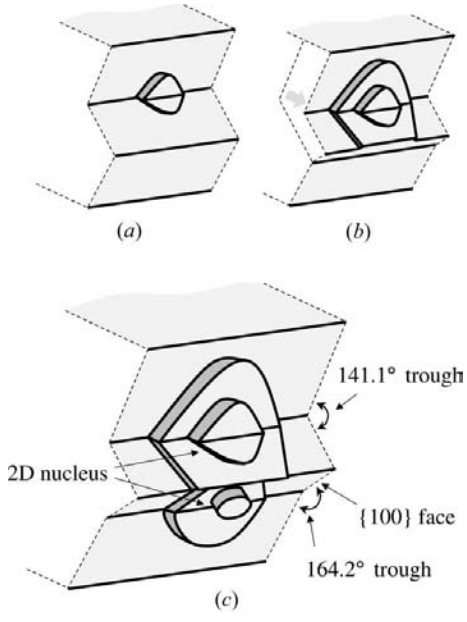

Figure 10
Schematics showing the modified TPRE mechanism contrasting with the original TPRE in Fig. 1. (*a*) The elliptical nucleus is formed on the {111}/{111} trough. (*b*) The nucleated layers accumulate around the ridge and form the {100} face. (*c*) 2D nucleation occurs on the {100} face in the middle crystal as well as the {111}/{111} trough.

References

Berriman, R. W. & Herz, R. H. (1957). *Nature (London)*, **180**, 293–294.
Bögels, G., Pot, T. M., Meekes, H., Bennema, P. & Bollen, D. (1997). *Acta Cryst.* A**53**, 84–94.
Bonzel, H. P. (2001). *Prog. Surf. Sci.* **67**, 45–58.
Chung, U. J., Park, J. K., Hwang, N. M., Lee, H. Y. & Kim, D. Y. (2002). *J. Am. Ceram. Soc.* **85**, 3176–3180.
Eerden, J. P. van der (1993). *Handbook of Crystal Growth*, edited by D. T. J. Hurle, Vol. 1A, pp. 307–475. Amsterdam: Elsevier.
Gilmer, G. H. (1976). *J. Cryst. Growth*, **35**, 15–28.
Hamilton, D. R. & Seidensticker, R. G. (1960). *J. Appl. Phys.* **31**, 1165–1168.
Hamilton, J. F. & Brady, L. E. (1964). *J. Appl. Phys.* **35**, 414–421.
Hilling, W. B. (1966). *Acta Metall.* **14**, 1868–1869.
Jagannathan, R., Mehta, R. V., Timmons, J. A. & Black, D. L. (1993). *Phys. Rev. B*, **48**, 13261–13265.
Jagannathan, R., Mehta, R. V., Timmons, J. A. & Black, D. L. (1995). *Phys. Rev. B*, **51**, 8655.
Lee, J.-W., Chung, U.-J., Hwang, N. M. & Kim, D.-Y. (2005). In preparation.
Lee, J.-W., Hwang, N. M. & Kim, D.-Y. (2003). *J. Cryst. Growth*, **250**, 538–545.
Li, H. & Ming, N. B. (1995). *J. Cryst. Growth*, **152**, 228–23.
Ming, N. B. & Sunagawa, I. (1988). *J. Cryst. Growth*, **87**, 13–17.
Ming, N. B., Tsukamoto, K., Sunagawa, I. & Chernov, A. A. (1988). *J. Cryst. Growth*, **91**, 11–19.
Pei, Y. T. & Hosson, J. T. M. D. (2001). *Acta Mater.* **49**, 561–571.
Sunagawa, I. (1987). *Morphology of Crystals, Part B*, edited by I. Sunagawa, pp. 509–587. Tokyo: Terra Scientific Publishing.
Sunagawa, I. & Yasuda, T. (1983). *J. Cryst. Growth*, **65**, 43–49.
Tiller, W. A. (1991). *The Science of Crystallization: Microscopic Interfacial Phenomena*, pp. 80–84. New York: Cambridge University Press.
Uyeda, R. (1987). *Morphology of Crystals, Part B*, edited by I. Sunagawa, pp. 367–508. Tokyo: Terra Scientific Publishing.
Waal, B. W. van de (1995). *Phys. Rev. B*, **51**, 8653–8654.
Waal, B. W. van de (1996). *J. Cryst. Growth*, **158**, 153–165.
Wagner, R. S. (1960). *Acta Metall.* **8**, 57–60.
Yoo, Y. S., Kang, M. K., Han, J. H. & Kim, D. Y. (1994). *J. Eur. Ceram. Soc.* **17**, 1725–1727.